Supporting Information

Tilted Magnetic Levitation Enables Measurement of the Complete Range of Densities of Materials with Low Magnetic Permeability

Alex Nemiroski[1], Siowling Soh[1], Sen-Wai Kwok[1], Hai-Dong Yu[1], and George M. Whitesides[1,2,3]*

[1]Department of Chemistry and Chemical Biology, Harvard University, 12 Oxford Street, Cambridge, Massachusetts 02138, United States.

[2]Wyss Institute for Biologically Inspired Engineering, Harvard University, 60 Oxford Street, Cambridge, Massachusetts 02138, United States.

[3]Kavli Institute for Bionano Science and Technology, Harvard University, 29 Oxford Street, Massachusetts 02138, United States.

*Corresponding Author: gwhitesides@gmwgroup.harvard.edu

Contents

SUPPORTING MATERIALS AND METHODS

Spherical objects

Spheres made of high-density polyethylene (HDPE), polyamide (nylon 6/6), polyamide-imide (Torlon), poly(tetrafluoroethylene) (Teflon), aluminum, silicon nitride, aluminum oxide, brass, and lead, were 1/8 inch in diameter, and were purchased from McMaster-Carr. The glass sphere was also 1/8 inch in diameter, and was purchased from Winsted Precision Ball Company.
Non-spherical objects

Non-spherical objects

Poly(tetrafluoroethylene) (Teflon), aluminum oxide, and lead were purchased from McMaster Carr. Minerals stibnite and cerussite were purchased from Alfa Aesar. Pieces of silicon, indium, copper, and silver were purchased from Sigma-Aldrich. Gold was purchased from VWR. Diamond was borrowed from Prof. Marko Loncar from the Harvard SEAS. Osmium and iridium were purchased from Metallium, Inc. For powders, gold powder (-100 mesh) was purchased from Alfa Aesar. Glass powder (150 – 212 μm), aluminum powder (-200 mesh), tin powder (20 mesh), and copper powder (-200 mesh) were purchased from Sigma-Aldrich.

Solutions

All manganese chloride ($MnCl_2 \cdot 4H_2O$) solutions (Alfa Aesar) used in this study had a concentration of 3.00 M. Some of the solutions were prepared by dissolving $MnCl_2 \cdot 4H_2O$ salt in aqueous solutions of dextran (average MW 5×10^5; purchased from Spectrum Chemical) with either 10%, or 35% by weight in a volumetric flask (the specific solution used is described in the main text). Some other solutions did not contain dextran; that is, these solutions contained only aqueous $MnCl_2$. Densities of various paramagnetic solutions were determined using a portable density meter (DMA 35, from Anton Paar). Paramagnetic solutions with 0%, 10%, and 35% dextran by weight and 3.00 M $MnCl_2$ have densities of 1.292, 1.319, and 1.385 g/cm^3 respectively.

When concentrated aqueous paramagnetic solutions of $MnCl_2$ or $GdCl_3$ were used, we were able to levitate objects up to a density of 1.7 g/cm^3 using NdFeB magnets.[1] When inorganic salts were added to the solution to increase the density of the solution, we could levitate objects up to a density of 2.3 g/cm^3 (e.g., using a 3.0-M solution $MnBr_2$ with 3.8-M $ZnBr_2$).[1] Because aqueous

salt solutions can reach a density of ~ 3 – 4 g/cm^3,[2] we presume that MagLev can—with appropriate preparation of the paramagnetic medium—be adapted to levitate objects up to ~3-4 g/cm^3 with the gravitational and magnetic fields coaxial.

Containers

We purchased square quartz cuvettes (dimensions of 10 mm × 10 mm × 45 mm) from Starna Cells, Inc., and cylindrical vials (15 mm x 45 mm) from VWR. We chose containers with a smooth inner surface (no roughness or embossed markings) because any unevenness prevented the object from moving toward the equilibrium position where $F_m = F_{g,z}$. We sealed the open end of the containers with parafilm.

Magnets

When measuring densities of the different objects listed in the main text, we used three different sets of magnets with slightly different magnetic strengths at the surface (and at the center) of the magnets: 0.380 T, 0.385 T, and 0.395 T. We determined these values with a Gaussmeter (Sypris, model 6010). In principle, denser objects can be levitated using stronger magnets. We used NdFeB magnets in this study because they are widely commercially available, inexpensive (each magnet costs ~ $5), portable (the device we use does not require additional equipment or external power), and simple to use. NdFeB also has a higher remanence compared to other permanent magnetic materials;[3] this characteristic is important to maintain magnetization even in the anti-aligned configuration.

Magnetic Susceptibilities

Table S1 shows the magnetic susceptibilities of the materials measured in this study. The magnetic susceptibilities reported here were all converted (when appropriate) from literature values (references in the rightmost column)[3-6] to unitless SI values. The magnetic susceptibility of air is negligible ($\chi_{air} \approx 0$) and is not included in this table. The magnetic susceptibility of the standard density bead χ_{bead} (with density ρ_{bead} = 1.8000 g/cm^3 reported by the manufacturer) used in Figure 4 (main text) can be estimated by Equation S1, which models the bead as a composite

object consisting of glass with density[7] $\rho_{glass} \approx 2.4$ g/cm^3 and susceptibility $\chi_{glass} = 1.39 \times 10^{-5}$, and an air pocket with negligible density $\rho_{air} \approx 0$ g/cm^3 and susceptibility.

$$\chi_{bead} \approx \chi_{glass}\left(\frac{V_{glass}}{V_{bead}}\right) \approx \chi_{glass}\left(\frac{\rho_{glass}}{\rho_{bead}}\right) \quad \text{(S1)}$$

Using this equation, we determined $\chi_{bead} = 1.04 \times 10^{-5}$.

Table S1. Literature values for magnetic susceptibility of samples

Material	Magnetic Susceptibility $\chi/10^{-6}$ (unitless)	Reference
High-Density Polyethylene (HDPE)	-9.69	4
Polyamide (Nylon)	-11.5	4
Polyamide-imides (Torlon)	- 6.51	6
Polytetrafluoroethylene (Teflon)	-10.6	4
Silicon	-3.25	3
Glass	-13.9	5
Aluminum	-20.7	3
Silicon Nitride	-9.0	5
Diamond	-21.8	3
Aluminum Oxide	-17.7	3
Stibnite (Sb_2S_3)	-14.6	3
Cerussite ($PbCO_3$)	-18.9	3
Indium	-8.16	3
Tin (white)	-2.4	5
Brass	-11.1	3
Copper	-9.65	3
Silver	-23.8	3
Lead	-15.6	3
Mercury	-28	5
Gold	-34.5	3
Iridium	-36.9	3
Osmium	-16.4	3

Literature Values of Densities

Tables 1-3 in the Main Text compare the densities measured using MagLev with the densities provided elsewhere. For objects made of high-density polyethylene (HDPE), polytetrafluoroethylene (Teflon), aluminum, silicon nitride, aluminum oxide, brass, or lead, the densities were provided by the manufacturer (McMaster-Carr). For glass, the density was obtained from literature.[7] We obtained densities of pure silicon, diamond, tin, indium, copper,

silver, mercury, gold, iridium, and osmium (all purchased with a purity of more than 99.9%) from the CRC Handbook of Chemistry and Physics.[3]. We obtained densities of the minerals stibnite and cerussite from the vendor (Alfa Aesar).

SUPPORTING EXPERIMENTAL DESIGN

Instruments and Measurement

When an object reaches the state $F_m = F_{g,z}$, the density of the object can be determined using Equation 4 (in the main text). Equation 4 requires the distance between the object and the surface of the bottom magnet, D_z, and the angle of tilt of the magnets, θ, to be measured. Figure S1 shows a schematic the experimental set-up.

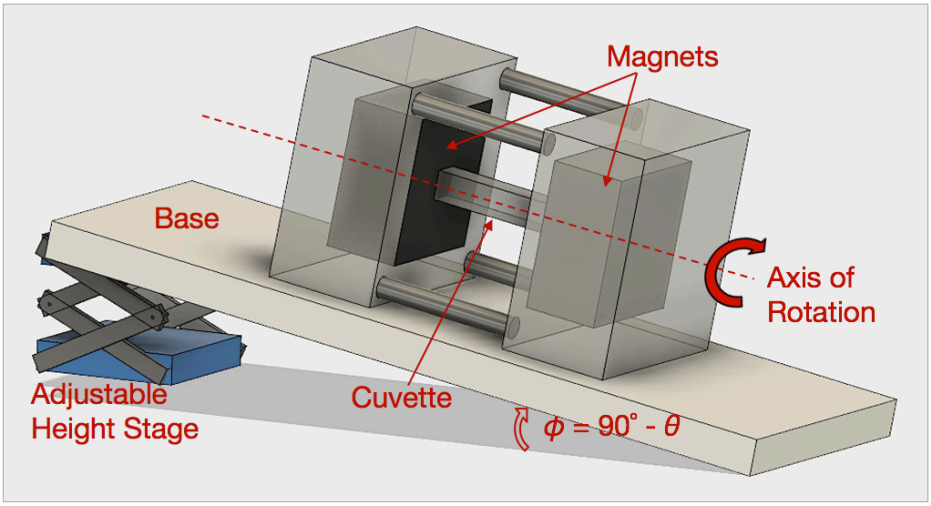

Figure S1. Experimental Set-up. We built a metal jig that held the magnets and cuvette in place. We then placed this jig onto a wooden base and adjust the angle $\phi = 90^\circ - \theta$ with a bubble level. When agitation was necessary, we lifted the jig manually, rotated it around the axis of rotation by successive quarter or half turns (depending on the application), and set it back down on the base between turns. When necessary, we repeated this procedure multiple times. In principle, a more sophisticated jig can be constructed to preserve the axis of rotation more accurately than is possible with manual manipulation of the MagLev device; in practice, however, we found that manual manipulation was sufficient to achieve a reproducible equilibrium position.

To determine these two parameters, we took images of the MagLev device with the object, after it reached the position where $F_m = F_{g,z}$. Our reference for θ was a bubble level; the straight edge of the level provided us with a horizontal line. Our reference for D_z was two fine lines drawn on a piece of paper. The outer edges of the two lines were measured by a vernier

caliper with accuracy of 0.01 mm; we used a microscope to aid us in adjusting the vernier caliper to measure the outer edges of the two lines. When an image was taken, it included both the bubble level, and the lines, together with the device and the object. Through using an image-processing software (Adobe Photoshop CS5), we determined amount of tilt, ϕ, by measuring the angle between the side of the vial (containing the object), and the horizontal edge of the bubble level. In our definition, we can calculate θ by $\theta = 90° - \phi$. We also used a digital angle indicator (a "digital precision level", McMaster-Carr, accuracy of 0.01°) to measure and check the values of θ. This digital level was capable of determining the horizontal plane automatically. When this digital level was placed on the side of the vial containing the object, it measured ϕ directly. For determining D_z, we measured the distance between the object and the surface of the bottom magnet using the image-processing software. By also measuring the distance between the outer edges of the fine lines (for which we know the exact real distance), we can convert the distance measured between the object and the surface of the bottom magnet from the units used in the image-processing software (i.e., pixels) into real units (i.e., millimeters).

Procedure for Measuring Densities of Objects with High Aspect Ratio

The method for measuring densities of non-spherical objects proposed in this study is dependent on the geometry of the object. In general, the variation in measurement is larger for an object with a higher aspect ratio. Consider, for example, a flat sheet falling from the top toward the bottom of the container. The object is observed experimentally (e.g., for the piece of diamond shown in the image on the upper left of Figure 2b in the main text) to fall in a direction that is biased according to the plane of inclination of the object (Figure S2a).

To better understand this effect, we performed a 2-D simulation of the liquid flow around a falling object (Figure S2b). Specifically, we modeled an object with dimensions of 3.6 mm by 0.2 mm (the size of the piece of diamond we used) within an enclosed domain of 15 by 15 mm. When the object is simulated to fall vertically downward (along the z-axis in Figure S2b) at a speed of 1 mm/s in a solution with viscosity 10 Pa.s and density 1385 kg/m^3, the x component of the force (arising from both pressure differences and shearing stresses) from the fluid acting on the object is positive, and is 0.02 N/m. A positive force in the x-direction pushes the object simulated in Figure S2b to the right — this result agrees with experimental observation. This

positive x component of the force accounts for ≈ 40% of the total force of the fluid acting on the object. This effect has also been observed and discussed in a previous study.[8]

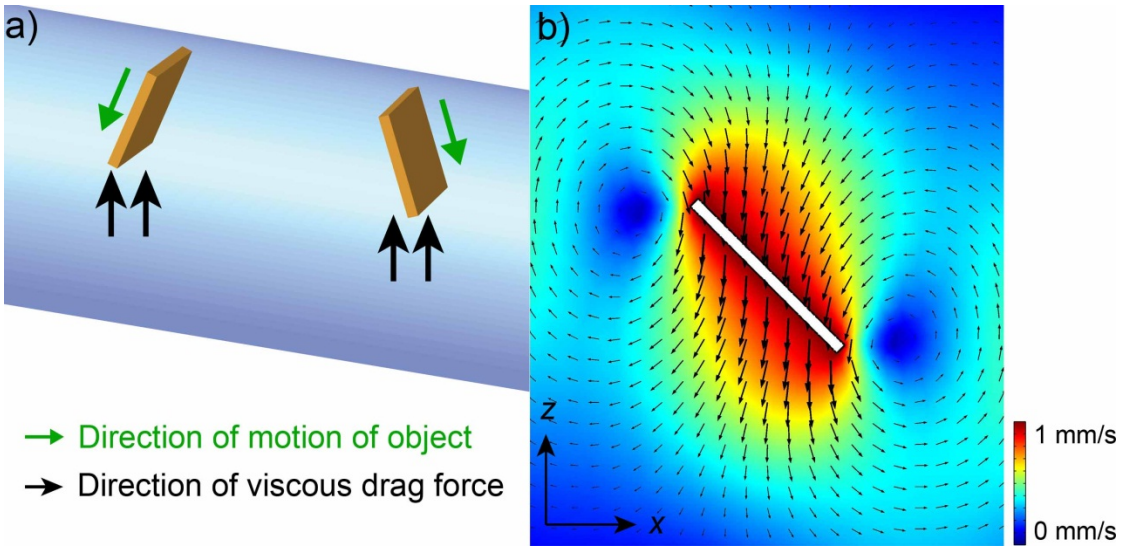

Figure S2. Simulation of motion and viscous drag on a flat object. (a) For a flat sheet, the direction at which the object falls within the solution is observed experimentally to be biased according to the angle of inclination of the object. Shown in this illustration are two flat pieces; an object inclined to the left will have the tendency to move to the left, and vice versa. (b) Simulated 2-D velocity profile of the fluid around a piece of object (with high aspect ratio) oriented at an angle of 45°, and falling down at a velocity of 1 mm/s.

The bias in motion arising from the inclination of the object could be overcome by rotating the container about the z-axis rapidly and continuously such that the object never came into contact with the walls of the container; that is, we did not allow the object to settle at the bottom surface of the container. Experimentally, we observed that with time, the flat sheet would gradually rotate such that the plane of the surface of the flat sheet became parallel to the surface of the magnet. Presumably, the magnetic force exerted a torque on the object; this torque rotated the object until it became parallel to the surface of the magnet.

This bias in motion due to shape was especially challenging for the case of osmium — the element with the highest known density, and an object with an irregular shape. It was not possible for us to rotate the container fast enough so that osmium did not come into contact with the walls of the container. In order to measure its density, we rotated the container more times than other objects (~100 times); more rotations were necessary before we were able to determine the equilibrium position (at $F_m = F_{g,z}$), where the object stopped moving along the z-axis.

Procedure for Determining Density of Gold Powder

The vial containing the gold powder and the paramagnetic solution was rotated 180° about the *z*-axis multiple times in order to move the powder to the position where $F_m = F_{g,z}$. Figure S3 shows how, initially, the powder was dispersed throughout the container due to the rotations (image on the left). With more rotations, however, the powder gathered into a narrower distribution (image on the right). This narrow band allowed us to measure the density of the gold powder.

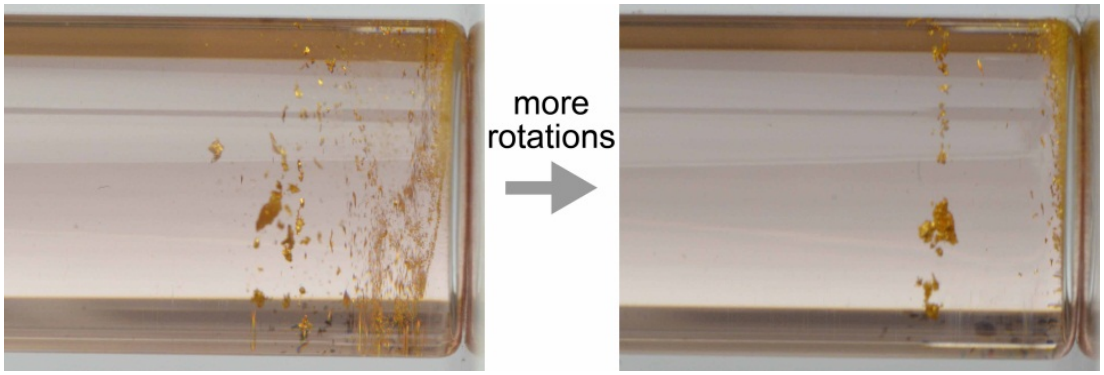

Figure S3. Image showing how continued rotations of the vial arranged a powdered gold sample into a thin region that with consistent distance to the bottom surface of the vial (seen hereon on the right side of the image).

SUPPORTING REFERENCES

(1) Mirica, K. A.; Shevkoplyas, S. S.; Phillips, S. T.; Gupta, M.; Whitesides, G. M. *J. Am. Chem. Soc.* **2009**, *131*, 10049–10058.
(2) Oster, G.; Yamamoto, M. *Chem. Rev.* **1963**, *63*, 257–268.
(3) *CRC Handbook of Chemistry and Physics*; Lide, D. R., Ed.; 76 ed.; CRC Press: Boca Raton, 2010.
(4) Van Krevelen, D. W.; Nijenhuis, Te, K. *Properties of Polymers: Their Correlation with Chemical Structure; their Numerical Estimation and Prediction from Additive Group Contributions*; Elsevier Science, 2009.
(5) Schenck, J. F. *Med. Phys.* **1996**, *23*, 815–850.
(6) Browning, V. M.; Soulen, R. J., Jr; Candela, G. A.; Eraker, J. H. *Cryogenics* **1996**, *36*, 391–393.

(7) Giancoli, D. C.; Boyle, J. J. *Physics: Principles with Applications*; 6 ed.; Pearson Prentice Hall: Upper Saddle River, 2005.
(8) Pulley, J. W.; Hussey, R. G.; Davis, A. M. J. *Phys. Fluids* **1996**, *8*, 2275–2283.